Cutting carbon emissions from China's food system by supply-demand coordination and optimizing spatial allocation of production

Xinxian Qi
Nanjing University
Xianjin Huang (hxj369@nju.edu.cn)
Nanjing University
Kuishuang Feng
University of Maryland, College Park https://orcid.org/0000-0001-5139-444X
Hong Yang
University of Reading
Taiyang Zhong
Nanjing University
Julian Thompson
University College London
Steffanie Scott
University of Waterloo https://orcid.org/0000-0002-4754-246X

Article

Keywords: food system, greenhouse gas emissions, food lifecycle, spatial heterogeneity, driver decomposition, mitigation pathways

Posted Date: May 18th, 2022

DOI: https://doi.org/10.21203/rs.3.rs-1648844/v1

Title page

Cutting carbon emissions from China's food system by supply-demand coordination and optimizing spatial allocation of production

Xinxian Qi [1,2], Xianjin Huang [1,2 *], Kuishuang Feng [3,] Hong Yang[4*], Taiyang Zhong[1,2], Julian R. Thompson[5], Steffanie Scott[6]

1. School of Geography and Ocean Science, Nanjing University, Nanjing, Jiangsu 210023, China

2. Key Laboratory of Carbon Neutrality and Territorial Space Optimization, Ministry of Natural Resources, Nanjing, Jiangsu 210023, China

3. Department of Geographical Sciences, University of Maryland, College Park, MD, 20742, USA

4. Department of Geography and Environmental Science, University of Reading, Reading RG6 6AB, UK.

5. Department of Geography, University College London, London WC1E 6BT, UK.

6. Department of Geography and Environmental Management, University of Waterloo, 200 University Avenue West, Waterloo, ON N2L 3G1, Canada

*Corresponding authors:

hxj369@nju.edu.cn (X. H.), h.yang4@reading.ac.uk (H. Y.)

Abstract:

Food systems, including supply chains, account for approximately one-third of global anthropogenic GHGs emissions. We construct a bottom-up GHG inventory of China's food system from farm to fork for the period 1990–2018. The decomposition method is used to assess regional differentiated drivers. GHG emissions reduced by 6.8% between 1990 and 2000 due to energy structure changes in East, Central and Southwest China. They then increased by 2.3% (2001–2010) because of rapid economic growth. Further large increases of 13.1% (2011–2018) were driven by growing consumption expenditure and GHG-intensive food consumption. In 2018 total emissions from China's food system, including supply chains, was 1.55 Gt CO_2e yr^{-1} (95%CI 1.07-2.03 Gt CO_2e yr^{-1}). Scenario simulation shows that demand- and supply-side synergies can offset emissions increases from high-quality protein food demands. Results demonstrate the importance of supply-side production spatial optimization and green source food importation for mitigating GHGs emissions.

Keywords: food system, greenhouse gas emissions, food lifecycle, spatial heterogeneity, driver decomposition, mitigation pathways

Agriculture and food production systems are responsible for over a quarter of global GHGs emissions (IPCC, 2014), while the entire food system (production, processing, distribution, preparation and consumption) accounts for approximately one-third (34% [25-42%]) of total anthropogenic GHGs (Crippa, et al. 2021). The emergence of food systems research provides a new paradigm for the comprehensive assessment of food-related resources and environmental effects (IPCC, 2019; Fan, 2021). These together support actions to achieve the UN's Sustainable Development Goals (SDGs) for zero hunger (Goal 2) and climate action (Goal 13) (UN, 2016). Calculations of food system GHG emissions provided by the NASA Research Institute (Rosenzweig et al., 2020) and EU Joint Research Center (Crippa et al., 2021) provide essential information to assess the trends and transition of global food system GHGs emissions, especially revealed the increasingly dominant GHG emissions in pre-and post-production processes along supply chains (Tubiello et al., 2022). To date, however, accurate food system emission inventories are still needed for regional-specific mitigation solutions. China, in particular, is the largest food system carbon emitter (Godfray et al., 2018), covers a vast territory that is characterized by heterogeneous environmental and socioeconomic conditions and is currently transitioning to high-quality diets (He et al., 2018; Zhao et al., 2021). Although estimated GHGs emissions per capita from China's food system (1.72 ton/capita) are still far below the global average (2.43 ton/capita; Crippa et al., 2021), the nation's food system is facing a profound transformation to meet future demands (Zhao et al., 2020) in the context of carbon neutrality and 1.5°C global warming targets (Roe et al., 2019).

The drivers of food-related GHG emissions, alongside measures through which they can be reduced, are related to both the demand- and supply-sides of the food system (Godfray et al., 2010; Poore and Nemecek, 2019). On the one hand, supply-side GHGs emissions can be reduced by closing the yield gap, promoting sustainable intensification and developing more efficient management practices (Zhang et al., 2013; Chen et al., 2014; Bajželj et al., 2014). On the other hand, food-related emissions ultimately depend on sustainable healthy diets from the demand-side (Heller and Keoleian, 2015; IPCC, 2022). These are influenced by dietary patterns and preferences (He et al., 2018; 2021; Hayek et al., 2021), especially for developed regions (Sun et al., 2022), food prices (Kehlbacher et al., 2016; Fujimori et al., 2022) and expenditure (Kramer et al., 1999). To sum up, mitigation of food system GHG emissions should therefore tackle both demand and supply, but such integrated approaches are currently lacking in China. Additionally, spatial optimization has received increasing attention and could play a significant role in some countries, including China, given the regional imbalances in resources and environmental problems (Jin et al., 2020; Bai et al., 2022).

To address knowledge gaps in region-specific food system GHGs inventories and investigate the mechanisms influencing food system emissions in China, this study provides the first attempt to build an approximate "bottom-up", from farm to fork, GHGs inventory at the provincial level for China's food system. This inventory is based on 12 types of food and almost 200 lifecycle processes. The study firstly extends understanding of regional "food-process-emission" linkages for China's food system and reveals the structural trends and characteristics of food system GHGs, including the contributions of different types of food to emissions. Secondly, the study decomposes factors influencing China's food system GHGs changes and downscales these factors with regional details. Thirdly, the study explores effective mitigation strategies and pathways for China's food system using five scenarios related to production technology upgrades, dietary shifts, domestic spatial allocation of production and international food imports. Our findings support policymakers to better understand GHGs emissions from China's food system and formulate tailored measures to cut these emissions.

Results

Structural shifts of food system and associated GHG emissions

Overall, China's food system GHGs emissions decreased between 1990 and 2000 but then increased up to 2018. Across the entire period 1990–2018, total GHGs from the Chinese food system increased from 1.44 Gt CO_2e yr^{-1} (95% confidence interval (CI): 1.00-1.88 Gt CO_2e yr^{-1}) to 1.55 Gt CO_2e yr^{-1}(95% CI: 1.07-2.03 Gt CO_2e yr^{-1}) (Fig. 1a; see Supplementary Table S2 for a detailed uncertainty description). China's food system emissions have undergone profound structural shifts in the dietary and supply chain stages as well as in their spatial distribution. In terms of dietary patterns, GHGs from China's food system has shifted from cereal-dominated foods in 1990 to highly carbon-intensive and more diverse foods in 2018 (Fig. 1a). Specifically, emissions from cereals reduced from 66.0% of the total in 1990 to 28.6% in 2018, while rice dropped from the top source of GHGs from the food system to the second but is still a significant source of CH_4 emissions (60.3% in 2018; Fig. 1c). Moreover, the carbon emission proportion from meat increased from 19.5% to 39.1%. Pork has been the leading and principal source of CO_2 emissions (Fig. 1c), increasing by 70.8% from 1990 to 2018 and accounting for 23.9% of total meat emission growth. Meat is another major source of CH_4 (34.3% of the total; Fig. 1c), with emissions being driven by manure management and fermentation from ruminant beef and mutton. Emissions from protein products have increased from 2.1% to 5.8%, whilst those from aquatic products have grown from 2.3% to 8.5% (Fig. 1a). Of the different GHGs, CO_2, CH_4, and N_2O accounted for 81.6%, 14.4%, and 4.0%, respectively, of China's overall food system GHGs in 2018. With the increasing demand for meat, the emissions from feed (wheat bran, soybean cake, corn) production and processing in the food supply chain rose from 94.5 Mt CO_2e yr^{-1} in 1990 to 193.0 Mt CO_2e yr^{-1} in 2018, 9.8% and 26.5% of the total emissions from food production, respectively (Fig. 1c, 1d).

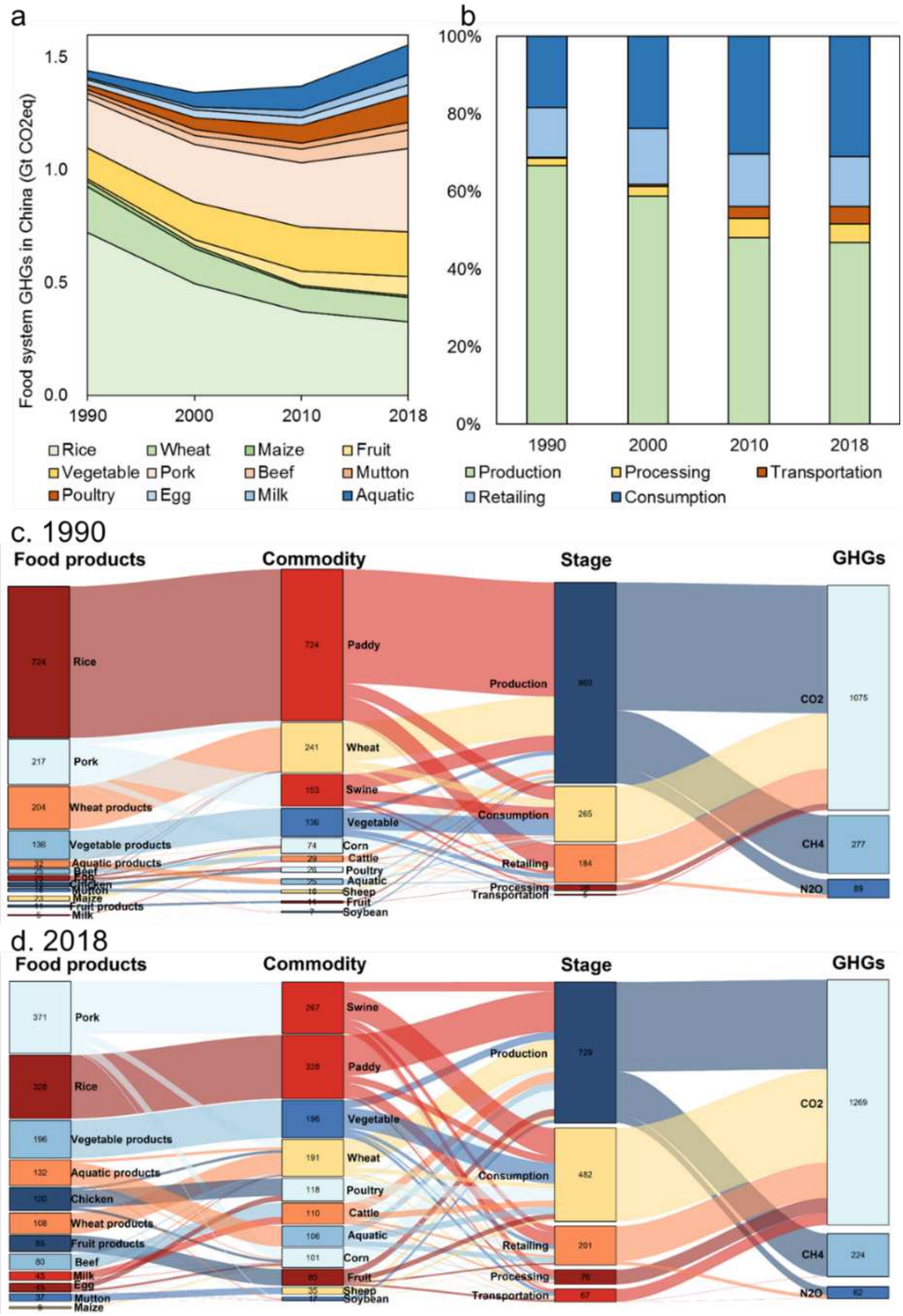

Figure 1. Structure of food system and associated GHG emissions. a. Total amount and food type structural changes in GHGs from China's food system during the period 1990-2018; b. structural changes in GHGs in China's food system at supply chain stages between 1990 and 2018; c. Sankey diagram of GHG emissions from the food system in China in 1990, representing the linkages among GHGs, food products, agricultural commodities and stages of China's food system GHGs; d. Sankey diagram of GHGs emissions from China food system in 2018.Between 1990 and 2018, the food supply

chain developed rapidly in China, leading to large emission changes from the post-production stage. During this period, the percentage of total GHG emissions associated with the post-production stage increased from 33.4% to 53.1% (Fig. 1b). In 2018, GHGs emissions from the production and preproduction stages accounted for 46.9% of the entire food supply chain, the consumption stage accounted for 31.0%, and processing, transportation and retailing accounted for 4.0%, 4.3% and 12.9%, respectively (Fig. 1b).

As the diversity of food consumption has increased, the proportion of cereals in the entire lifecycle stage has decreased. Conversely, the proportions of fruit, vegetables, meat (pork, mutton, beef, and poultry), protein products (milk and eggs) and aquatic products (fish, shrimp, crab, shellfish, and algae) have increased, especially in the post-production stage. The relative importance of GHG-intensive foods rose from 25.6% in 1990 to 55.2% in 2018 (Fig. S4). At the production stage, cereals dominated GHGs emissions, but their contribution reduced from 74.2% in 1990 to 38.0% in 2018. Meat and protein food increased from 22.9% to 51.3% during the same period. Rice and pork dominated the structural changes declining from 56.8% to 28.8% and rising from 14.4% to 20.8%, respectively (Fig. S4). Over the period 1990–2018, significant reductions in N fertilizer (-91.8%) and paddy CH_4 emissions (-40.6%) contributed to a very large decline in GHGs from the production stage of rice (Fig. S6). However, these two sources still contributed the largest emissions at the end of this period (38.0% and 12.0%, respectively, with an additional 11.7% being contributed by straw burning). For the production emissions from pork, forage production (28.2%), energy use (9.4%) and manure management (9.1%) were the three primary GHG sources at the production stage in 2018. Although the emissions of energy use in the production stage of pork were reduced by 75.4% between 1990 and 2018, overall production emissions increased by 12.9 Mt CO_2e yr^{-1} (9.3%) due to an increase of 59.0% from forage planting (Fig. S6)

In the processing stage, pork slaughtering accounted for the majority (56.0%) of emissions (Fig. S4), rising by 31.5 Mt CO_2e (2.9 times) between 1990 and 2018 (Fig. S5). For the transportation stage, vegetables contributed the largest proportion of national food system transport emissions, accounting for 28.2% in 2018 (Fig. 4), increasing almost 12.0 times from 1990 (Fig. S6). At the retail stage, rice, pork, aquatic products and vegetables accounted for 72.1% of the total national retail stage emissions in 2018. In the consumption stage, pork accounted for 29.3% of the total consumption emissions in the same year (Fig. S6), increasing by 88.5 Mt CO_2e (1.7 times) from 1990 (Fig. S6). The proportion of highly carbon-intensive food, such as meat, protein foods and aquatic products, accounted for 59.0% of total consumption stage emissions in 2018, increasing from 29.4% in 1990 (Fig. 1b, Fig. S5).

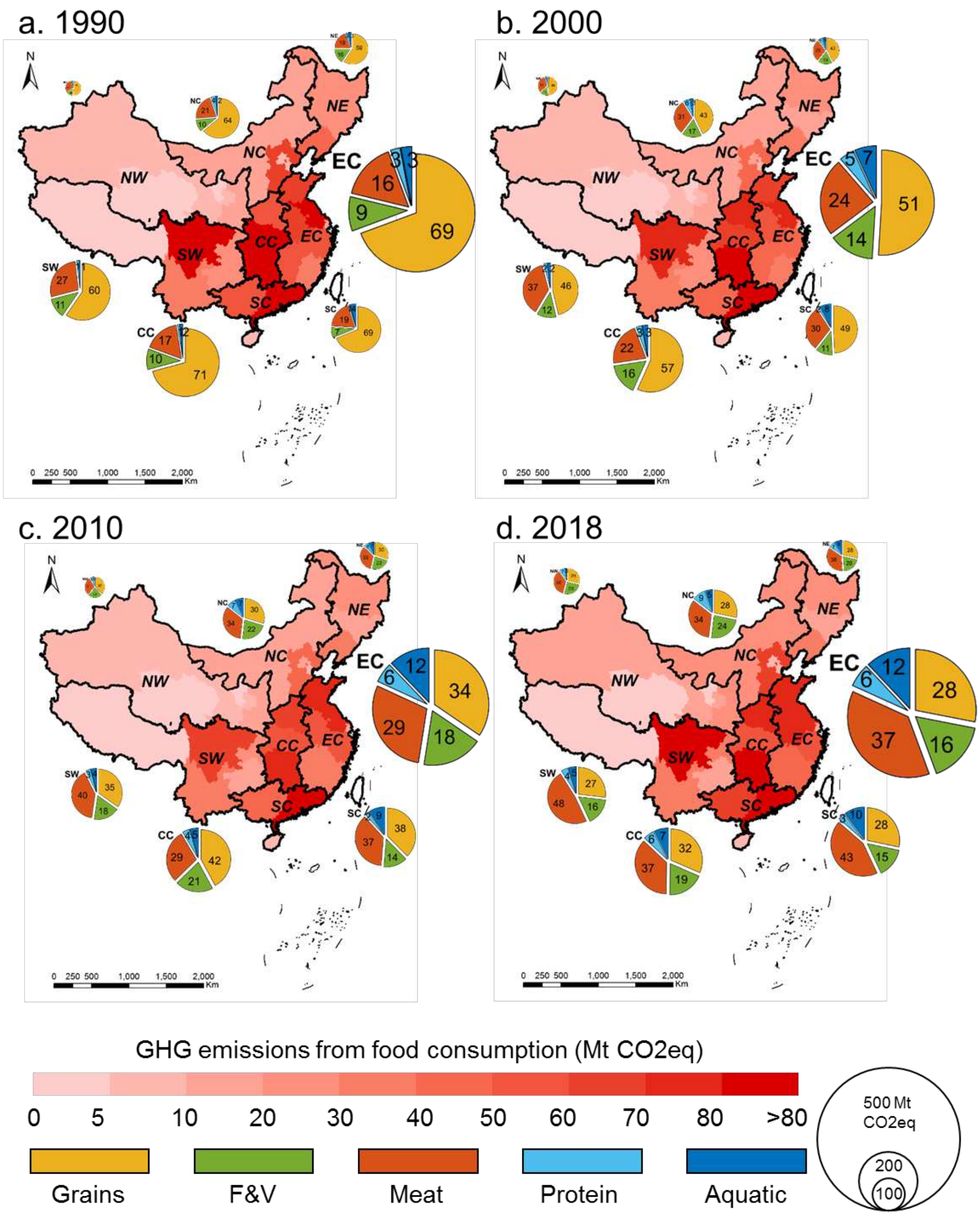

Figure 2. Spatial distribution and consumption patterns trends of food system GHGs from 1990 to 2018. Different shades of red on the maps represent changes in total GHGs

from regional food systems. Colors in the pie charts represent different food types with numbers representing percentages of the total. The sizes of pie charts correspond to emission amounts. Grains comprise rice, wheat, and maize; F&V comprise fruit and vegetables; meat comprises pork, beef, mutton, and poultry; protein comprises eggs and milk; and aquatic comprises fish, shrimp, crab, shellfish, and algae etc. NE = Northeast China, NC = North China, NW = Northwest China, EC = East China, SC = South China, CC = Central China, and SW = Southwest China.

Spatially, GHG emissions from China's food system were primarily concentrated in the south. The contribution of the southern part of the country (here comprising four regions: EC-East China, SC-South China, CC-Central China, and SW-Southwest China) to the national total GHGs decreased slightly from 77.0% in 1990 to 75.4% in 2018 (Fig. 2d and Fig. 2a). Total GHGs emissions from the food system in East China were the highest, accounting for 30.3% of the total national emissions, followed by South China with 16.0%. In contrast, Northwest China accounted for the lowest, only 6.1% in 2018. In terms of the change rate between 1990 and 2018, GHGs from food systems increased in both the southern and northern regions, but the latter experienced a more rapid growth rate (on average 15.2% in the north compared 6.2% in the south. Northwest China (NC) had the most rapid growth rate (68.8%), while Southwest (SW), Central (CC), and Northeast China (NE) experienced decreasing trends (3.5-6.7%).

In terms of the spatial characteristics of GHGs emissions from different types of food, in most cases, with the exception of mutton, emissions from the south were higher than those from the north. From the perspective of dietary structural change, all regions showed a unified trend of decreasing GHGs emissions from cereal food and increasing emissions from fruit and vegetables, protein foods and aquatic products. However, there was significant spatial heterogeneity in emissions caused by regional dietary structure changes. Food system GHGs increases in South China were dominated by meat, those in North China were primarily from meat and vegetables, whilst those in East China were led by aquatic products (Fig. 2). As the largest food system GHGs emitter in the country, East China experienced the largest drop in cereal related emissions (-58.1%) and a large increase in meat (21.8%) and aquatic product (9.0%) emissions over the period 1990–2018 (Fig. 2). In South China, high carbon-intensive meat consumption caused this region to experience the largest emission growth rate in the country. GHGs from meat consumption rose by the largest amount (219.4%), and the percentage of GHGs from meat increased from 19.0% in 1990 to 43.3% in 2018. In Northwest China, the large growth rate in food system GHGs emissions between 1990 and 2018 were dominated by meat (2.1 times) and vegetables (near doubling) (Fig. 2).

Overall food GHGs emissions per capita experienced an initial decline between 1990 and 2010 followed by an increase, reaching 1.11 tons per person in 2018 (Fig. S7). The highest GHGs per capita are in South China (1.45 tons per person in 2018) and exhibited a gradual increasing trend since 2000 (9.8% over the growing period). GHGs per capita in Northwestern China increased by 30.6%, while those in other regions decreased, with East China experiencing the largest declines of 17.0% (Fig. S8). For GHGs emissions per capita in 2018, grains were responsible for the largest emissions in South China, fruits and vegetables provided the largest emissions in North and Northwest China, while in South China meat was responsible for the largest emissions. Protein products provided the largest proportion of emissions in North China, whilst in East and Southeast China this role was dominated by aquatic products (Fig. S8, S9).

Drivers of food-related GHGs emissions

To quantify the relative contributions of multiple drivers to total food system GHGs emissions, we used Log Mean Divisia Index (LMDI) decomposition analysis to decompose the GHG changes in various food types in each region into eight factors. These factors comprise one supply-side driver (technology), four demand-side drivers (food consumption structure, food purchasing power, Engel coefficient, and expenditure), and three socioeconomic drivers (economic growth, urbanization and population; Fig. S9). Overall, economic growth (contributing 173.2% of the growth) and food purchasing power (contributing 136.0% of the reduction) had the largest impacts on China's food system GHGs emission during the period 1990–2018. The Engel coefficient contributed 57.8% to the decrease in GHGs emissions, whilst shifts in dietary pattern contributed 30.7% to the increase in these emissions. Changes in GHGs emission intensity contributed 28.4% of the decrease in food GHGs, while expenditure and population contributed 23.9% and 20.2% of the increases, respectively. For the whole country, the impact of urbanization was relatively small, with a cumulative impact of only 0.7%, but the influences of urbanization varied between different regions and different food types (for more details of the downscaling decomposition in Fig. 5 see Fig. S12).

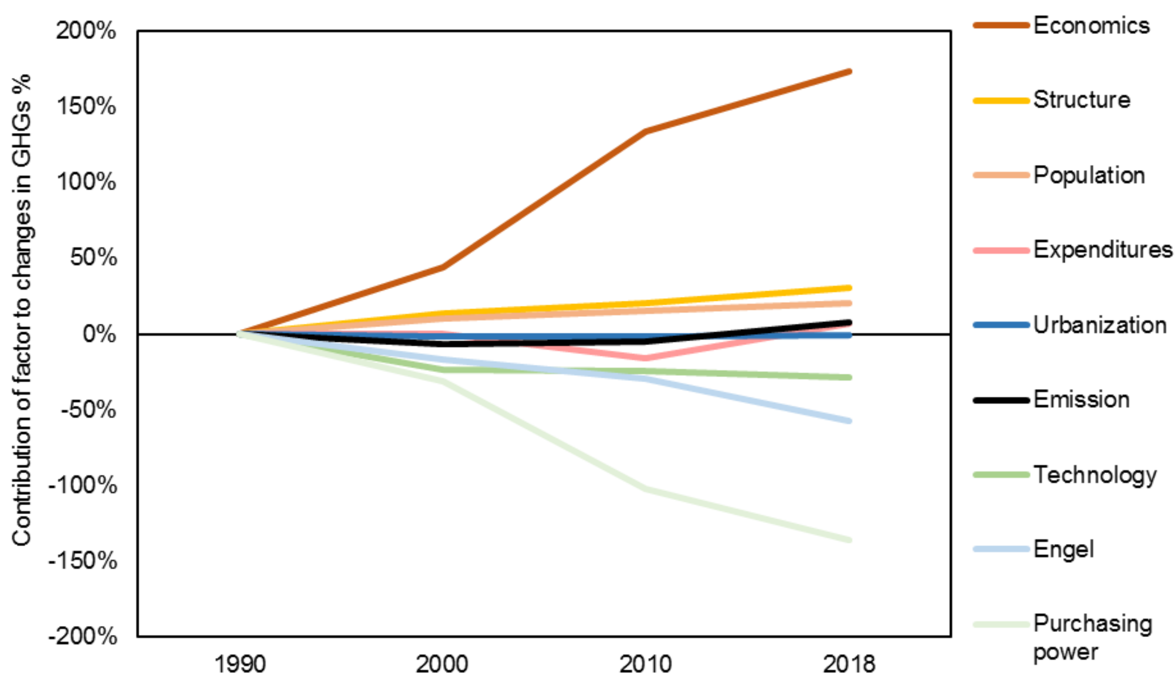

Figure 3. Contributions of different factors to changes in food system GHGs between 1990 and 2018. Using 1990 as the base year, the solid black line shows the percentage change in total food system GHGs. The other lines show the contribution to the change in emissions from eight different drivers.

Between 1990 and 2000, a period that was associated with achieving sufficient food for the Chinese people, GHGs emissions from China's food system decreased by 6.8% (Fig. 4). The reduction in emission intensity (technology) of 9.8% was the main reason for the overall reduction in food system GHGs during this phase. Optimization of the energy structure of the food system in East, Central and Southwest China (Fig. 4, S11) resulted in reduced use of raw coal in the processing of cereal (e.g. wheat and maize) and rice (Fig. S12). Economic growth, consumption structure and population growth contributed 43.7%, 13.4% and 10.0% to the overall growth, respectively, while the Engel coefficient and food purchasing power contributed 16.6% and 31.7% to the decrease, respectively (Fig. 4). Food purchasing power contributed the most to the declines in East China for all food types (Fig. S11 and S12).

During the period 2001–2010, a stage associated with progress toward more comfortable standards of living for many Chinese people, the direction of change in China's food system GHGs reversed with overall increases, albeit of relatively small magnitude (2.3%, Fig. 4) taking place. Economic growth played the largest role in this period, contributing 96.9% of overall growth and being particularly important in East

China, Central China, South China and Southeast China, (Fig. 4, S11). China's per capita gross domestic product (GDP) increased from 1,222 USD in 2000 to 4,740 USD in 2010, an almost 3-fold increase. Other increases were due to consumption structure transformation (7.4%), population growth (6.0%) and emission intensity (technology), although the influence of the latter weakened (0.7%) compared to the previous period. Reductions in consumption expenditure and food purchasing power contributed 17.0% and 75.8% to the decreases but these could not offset the growth brought about by the other drivers.

Between 2011 and 2018, a period with widespread comfortable living standards, GHGs emissions from China's food system continued to increase with an overall growth of 13.1% (Fig. 4). Transformation of consumer expenditure contributed 23.9% of the increase and was particularly concentrated in Central, East China, and North China (Fig. 4, S11). The increasing effect of the transformation of the dietary pattern contributed 10.9% of the growth and was focused, in particular, within the developed areas in East, Central, Southwest, and South China (Fig. 4, S11). A total of 86.6% of the emission increase by consumption structure was related to GHG-intensive consumption of meat, protein foods and vegetables (Fig. S12). In addition, economic growth contributed 41.1% of the GHGs increase. While the reduction in GHGs from the food system due to the Engel coefficient increased to 29.4%, the food purchasing power effect on the reduction in food system GHGs decreased by 35.4%. The impacts of emission intensity (technology) on GHGs emission reductions declined in all regions and even reversed (i.e. increase in GHGs) in North and Northwest China (Fig. 5 and Fig. S11).

There were apparent spatial variations in the effects of the different drivers on food system GHGs emissions. The impacts of urbanization were relatively small (3.9% decrease overall) (Fig. 3) but continued to increase in Northwest and North China with the influence direction in Northeast, East and South China switching from decreases to increases (Fig. 4, S10). In particular, within the highly urbanized South and East China, the impacts of urbanization on food system GHGs emission decreased in the first two periods described above (1990–2000 and 2001–2011) then increased between 2011 and 2018 (Fig. S11). Increases in GHGs emissions driven by population gradually weakened in all regions (Fig. 5), especially in Northeast China; in the final period the population even had a decreasing effect (Fig. S11).

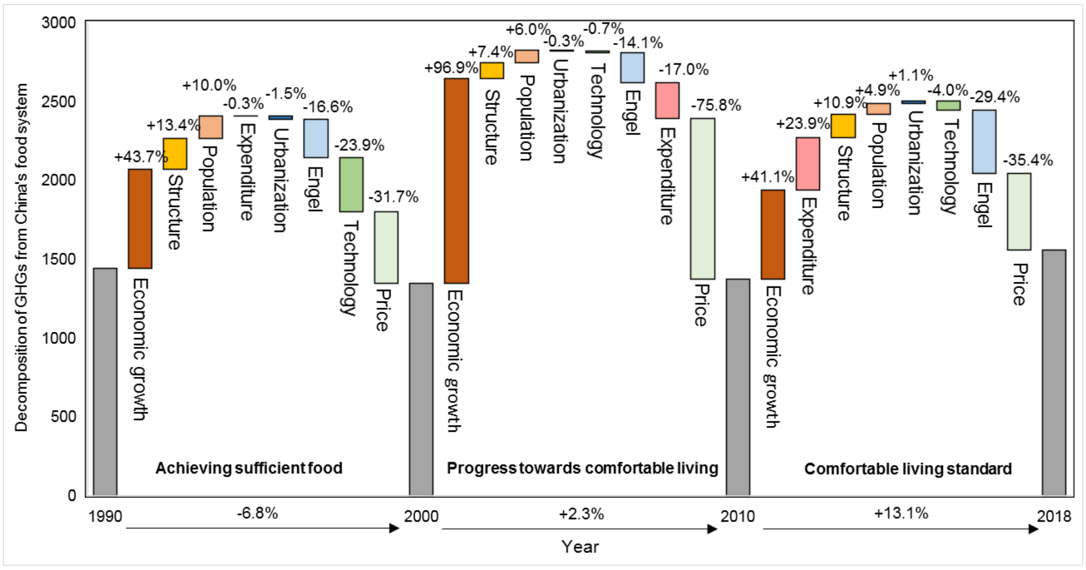

Figure 4. Contribution of different factors to the changes of GHGs in food system in three periods. According to the classification standard of the Engel coefficient used by the FAO these periods are 1990–2000 - achieve sufficient food, Engel's range 50%–59%; 2001–2010 – progress towards comfortable standards of living, Engel's range 40%–49%; and 2011–2018 – widespread comfortable living standards, Engel's range 30%–39%.

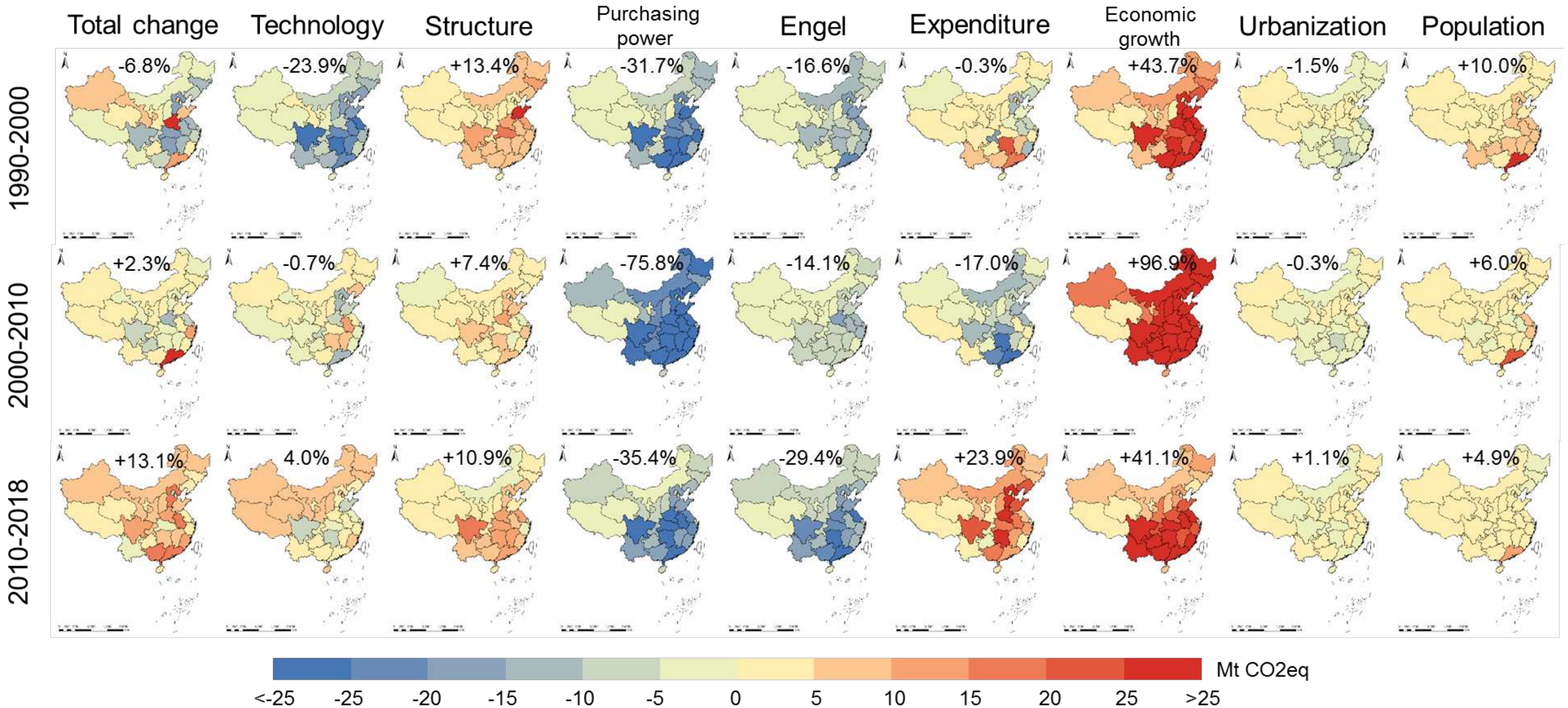

Figure 5 Spatial patterns in total food system GHGs emissions changes and the role of eight drivers between 1990 and 2018 in China. Percentage values indicate the contribution made by each driver to overall.

Mitigation pathways for China's food system GHGs emissions

Five scenarios were constructed to project China's food system GHGs emissions to 2060: the S0 business-as-usual scenario (BAU) basically following the SSP2, S1 production technology upgrade (TECH), S2 dietary pattern transformation (DIET), S3 domestic optimizing spatial allocation of crops production (SPAT), and S4 international import pattern optimization (IMP) (see Methods and Supplementary Table S4 for detailed description of the scenarios). All potential changes for S1-S4 are compared to BAU for the same year and the numbers in brackets after these figures in the following discussion represent the uncertainty of each scenario. Results show that S2 DIET, the transformation of the nutrient-oriented dietary pattern, will lead to a 14.9% decrease in the food system GHGs emission, whereas it has the highest emission reduction potential (43.0%) by 2060 (Fig. 6a). Due to demand for high-quality protein food, vegetables and fruit, and the lack of a "healthy-sustainable" dietary guide for the Chinese population, the emission reduction potential of the transformation of the food consumption structure is highly uncertain (-43.0% - 7.3%). S1 TECH, which focusses on upgrading food production technology, also has a high emission reduction potential of 12.1% (-16.3%, -7.9%). Comparison between the S3 SPAT domestic production and S4 IMP imports scenarios indicates that the former can achieve more effective emission reduction (-3.5% (-3.0%, -3.9%)) than the latter (-2.7% (-1.2%, -4.3%)). The spatial optimization of domestic grain production is a sustainable path to reduce the rising emission potential for the vulnerability of international agricultural markets.

The emission reductions at the supply-side can be further enhanced by both technological upgrades and spatial optimization. The combined emission reduction effects of S1 and S3 are equivalent to 212 Mt CO_2e (13.8%) over the BAU (Fig. 6b). A combination of measures at production and consumption sides can systematically reduce emissions. The combination of S1 and S2 can achieve approximately the same reduction over the baseline scenario, which means the upgrading technology could offset the emission increase from high quality food consumption, but with considerable uncertainty without a "healthy-sustainable"" dietary guide (Fig. 6b). The comprehensive optimization of domestic and international production space can also contribute to reducing Chinese food system GHGs emission; combining S3 and S4 produces a decline of approximately 92 Mt CO_2e (6.0%) over the BAU (Fig. 6b).

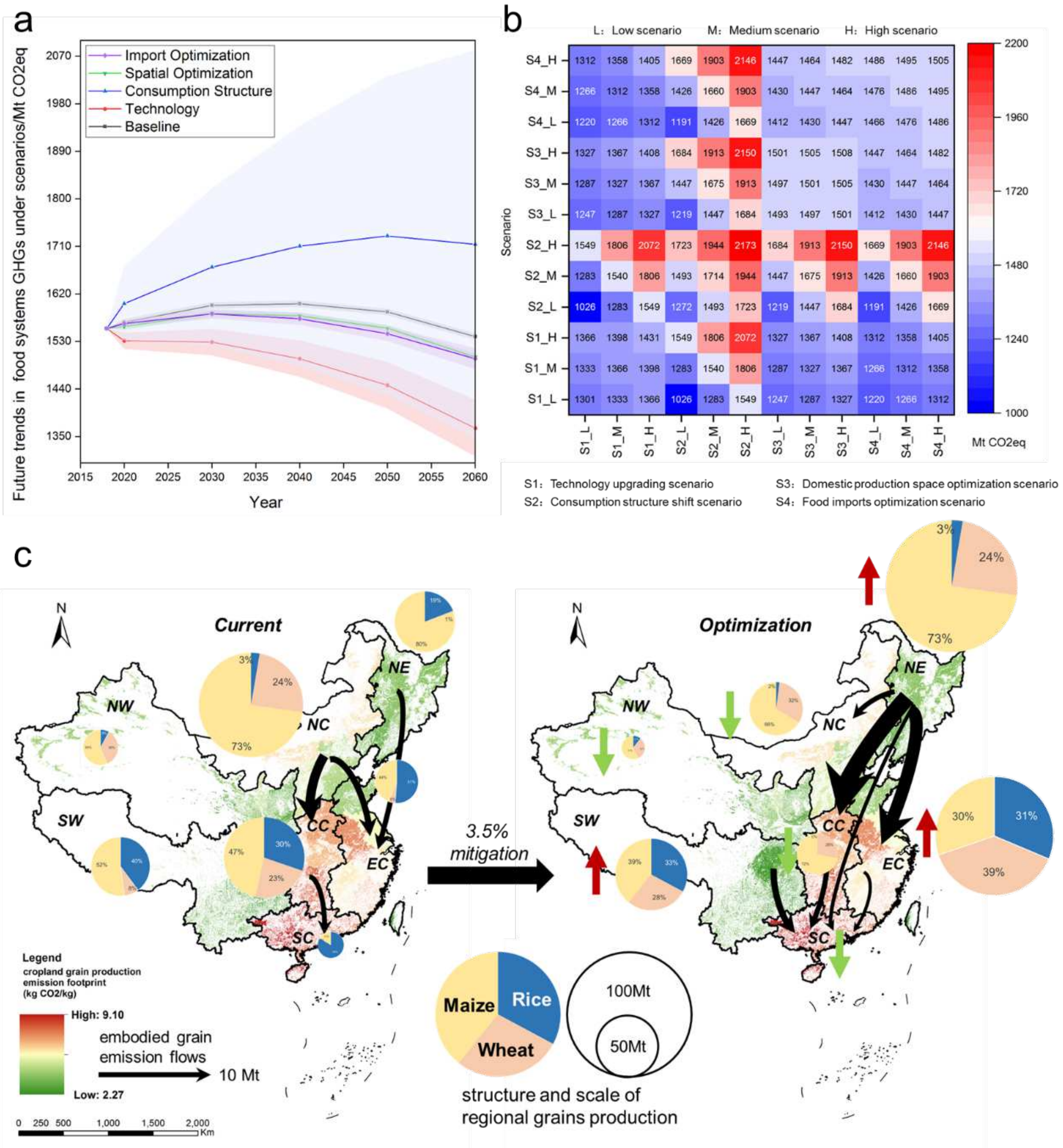

Figure 6. Mitigation pathways of China's food system GHGs emission. a. Food system GHGs emissions in China for five scenarios between 2018 and 2060. The colored lines represent the trend of each scenario and the shaded areas represent the uncertainty for each scenario. b. Combined effects of scenarios in 2060 for GHGs from food systems. The value and color of each grid represent the effect combined by the column and raw scenario. c. Spatial optimization process of grain production, current situation on the left and the optimization on the right, the color of the map represents the emission footprint of grain production in different regions, the pie chart represents the structure and scale of regional grains production, black arrow represents the inter-regional grain embodied emission flows, the red arrow represents the increase of grain production while the green arrow represent the decrease.

Discussion

The food system framework breaks down entrenched sectoral categories within the national GHG inventory framework described by IPCC (2006) (Rosenzweig et al., 2020). However, novel practical frameworks for understanding food system GHGs are required (IPCC, 2019). With the booming development of food supply chains (Garnett, 2011) and increasing importance for food supply chains to adapt to climate change (Gustafson et al., 2021), supply-related emissions have gradually been incorporated into the food system emission accounting (see Supplementary Table S2 for a detailed comparison of different results). Although different datasets and methodologies provide varying accounting results for food system GHGs, there is a consensus within the existing literature that food systems, including the complete supply chain, account for approximately one-third of anthropogenic GHGs (Crippa et al., 2021). Nevertheless, inconsistent and poorly defined system boundaries could lead to significant accounting bias (Rosenzweig et al., 2021). Additionally, it is essential to incorporate food system GHGs into nationally determined contributions (NDCs) rather than just the previously considered agriculture, forestry, and other land use (AFOLU) category (Rosenzweig et al., 2021). It is also urgent that regional mitigation pathways need to be developed. These require that the inventories not only contain specific information on consumption-oriented food patterns but consider regional and other scales of spatial heterogeneity.

Within this study, the provincial food type-specific “bottom-up” GHG inventory of China's food system is an exploration of such regional downscaling. This research addresses the gap in regional lifecycle emission estimations and driver differentiation for the nation’s food systems. Results demonstrate that reduced use of raw coal in the production stage for cereal in East, Central and Southwest China largely drove reductions in food system GHGs emission between 1990 and 2000 (Figs. S9 and S10). However, with the development of the food supply chains, the post-production stages have become increasingly dependent on energy (Tubiello et al., 2021). This will necessitate cleaner energy supplies to mitigate the impacts of energy-dependent food supply chains. In line with Garnett (2015), but including regional details, this study found that economic growth was the most dominant factor driving the increases in China’s food system GHGs. It was crucial in East, Central, South and Southeast. The rapid growth rate of China's food system GHGs since 2011 was primarily led by consumer expenditure increases in Central, East, and North China as well as shifts in dietary patterns, principally associated with GHG-intensive meat and protein food, especially in the more developed areas in East, Central, Southwest, and South China.

The multi-side "supply-demand" factor decomposition model was constructed to systematically analyze the influencing mechanisms driving changes in GHGs emissions from China's food system. Although it has been argued that the global supply mitigation potential is greater than that of the demand-side (Rosenzweig et al., 2020), quantitative evidence from this study shows that the reduction effect caused by demand-side factors had a larger potential compared to supply-side factors (Table S3). It was, however, demonstrated that supply-demand cooperation provides a more effective and substantial pathway to reduce China's food system GHGs emissions (Fig. 6b). The food purchasing power mechanism plays an important role in national emission mitigation and varies from region to region. Results of this study could, therefore, provide evidence for regionally differentiated food carbon tax policies. Frank et al. (2019) suggested that a food carbon tax specifically reflected in food prices could reduce global GHGs by 8% by 2050. Carbon tax-based redistributed compensation mechanisms in China would permit the inclusion of regional differences in order to prevent risks of hunger and malnutrition, which could otherwise result from spatially uniform emission mitigation policies (Hasegawa et al., 2018; Soergel et al., 2021).

Although China's food system emissions are still far below the global average (Crripa et al., 2021), the country should take responsibility in proposing more ambitious mitigation measures along with pursuing high-quality food consumption. China has promulgated the health-oriented Dietary Guidelines for Chinese Residents (2016), but such guidelines lack consideration of their potential environmental impacts (Supplementary S3.4). Therefore, there is an urgent need to develop "healthy and sustainable" co-benefit dietary guidance to promote environmentally friendly diets, shifting the food system from the demand-side to the supply-side. Previous studies have demonstrated that a combination of supply- and demand-side policies has synergistic effects (Sprinmann et al., 2018; Poore and Nemecek, 2018). Our study shows that supply-side technological upgrades can offset increased GHGs emissions from the demand-side of high-quality protein foods. Of course, in the globalization context, the effect of international food imports on domestic food GHGs cannot be ignored (Zhao et al., 2020). This study simulated a scenario in which China imported carbon-intensive food from green source agricultural exporting countries with low-carbon production practices, demonstrating a 41.9 Mt CO_2e (2.7%) reduction in emissions (Supplementary

S3.5). Compared with a limited import mitigation strategy, the optimization of food production allocation for grains has a relatively higher 3.5% mitigation potential to against the instability of international food trade, which could provide a new solution through production spatial redistribution as a land-based climate change mitigation measures (Fujimori et al., 2022). For instance, as simulated using the low-carbon oriented spatial equilibrium model assuming optimization through planting loation adjustment by spatial planning and development of low-carbon intensive unused cultivated land, demand driven rice expansion in the future could be distributed in the currently unexploited land in Northeast China and the Yangtze River Delta, with low-carbon production practices and overall low-carbon emissions from the supply-side (Supplementary S3.4). Our novel findings of domestic production optimizing strategy also provide insights into the dual-challenges of food security and climate change in an unstable global environment. In particular, the Ukraine war has threatened the stability of world food supplies (Nature Editorial, 2022). Approximately 84.3% of China's maize was imported from Ukraine and Russia (FAOSTAT), while the supply crisis with maize could be addressed, at least temporarily, by reclaiming domestic unused cropland in low-carbon northern regions in China. However, this optimization result is limited to the full consideration of scarce resources, such as water resource, in northern regions of China.

Methods

LCA and system boundary of the food system

Life Cycle Assessment (LCA) is the evaluation of the environmental burdens associated with a product, process, or activity. It is based on identifying and quantifying the energy and materials used and, in turn, the waste materials released into the environment (Garnett, 2008). The International Organization for Standardization (ISO) has standardized this framework within the ISO 14040 series on LCA. The LCA of the food system includes the entire lifecycle of food, encompassing preproduction, production and post-production processes.

The food system assessed in this study involves 12 primary food categories consumed by Chinese people and comprises five plant-sourced foods (rice, wheat, maize, vegetables, and fruit), seven animal-sourced foods (pork, beef, mutton, poultry, egg, and milk), and aquatic foods (fish, shrimp, crab, shellfish, and algae). The nutrients supplied from these 12 food categories account for 85.4% of the total calories and 88.7%

of protein intake by Chinese people (FAOSTST, 2019). Following the EU (2020) Farm-to-Fork Strategy, the food supply chain includes preproduction (extraction of the resources needed to produce agricultural products), production (the land and farm management practices by farmers during the food production process), and post-production (processing, transportation, packaging, distribution, retail, household refrigeration and cooking) (Fig. S1, S2). Emissions from land use and land use change (LULUC) associated with agriculture in the preproduction stage were excluded from the assessment since it is difficult to link them directly to the food lifecycle, the basic framework employed in this study (Lai et al., 2016). Post-consumption stages (food waste and disposal) were not considered owing to their high variability and low food-specific data availability (Xue, et al., 2021). Supplementary S1.2 justifies other exclusions.

Decomposition analysis

The LMDI method, developed by Ang (2004), was used to analyze how supply- and demand-side drivers affect food system GHGs structural shifts in China. LMDI quantifies the contribution of each driving force in proportion without residuals. To conduct the decomposition analysis, the GHG changes for the different food types in each region were decomposed into eight factors: technology, food consumption structure, food purchasing power, Engel coefficient, expenditure, economic development, urbanization and population.

$$FE_{Total} = FE_U + FE_R \qquad \text{Equation 4-1}$$

$$\begin{aligned} FE_U = \sum_{i,j} \frac{FE_{U.i,\mathrm{j}}}{Con_{U,i,j}} * \frac{Con_{U,i,j}}{Con_{U,j}} * \frac{Con_{U,j}}{FEXP_{U,j}} * \frac{FEXP_{U,j}}{EXP_{U,j}} \\ * \frac{EXP_{U,j}}{GDP_{U,j}} * \frac{GDP_{U,j}}{P_{U,j}} * \frac{P_{U,j}}{P_j} * P_j \\ = \sum_{i,j} EI_{U,i,j} * CS_{U,i,j} * CP_{U,j} * EN_{U,j} \\ * CE_{U,j} * ES_{U,j} * UR_{U,j} * P_j \end{aligned} \qquad \text{Equation 4-2}$$

$$FE_R = \sum_{i,j} \frac{FE_{R.i,\mathrm{j}}}{Con_{R,i,j}} * \frac{Con_{R,i,j}}{Con_{R,j}} * \frac{Con_{R,j}}{FEXP_{R,j}} * \frac{FEXP_{R,j}}{EXP_{R,j}} * \frac{EXP_{R,j}}{GDP_{R,j}} * \frac{GDP_{R,j}}{P_{R,j}} * \frac{P_{R,j}}{P_j} * P_j = \sum_{i,j} EI_{R,i,j} * CS_{R,i,j} * CP_{R,j} * EN_{R,j} * CE_{R,j} * ES_{R,j} * UR_{R,j} * P_j \qquad \text{Equation 4-3}$$

where *i* denotes the different food types, *j* denotes the different Chinese provinces, U denotes urban factors, and R denotes rural factors. FE_{Total} are the total GHGs emissions from the food system in China, and FE_U and FE_R are the GHGs from urban and rural residential consumption, respectively. $FE_{U.i,\mathrm{j}}$ denotes the urban residential consumption GHGs of food i in province j, $Con_{U,i,j}$ denotes the urban residential consumption volume of food i in province j, $Con_{U,j}$ denotes the urban residential consumption volume of all food types in province j, $FEXP_{U,j}$ is the food consumption expenditure of all types of food in province j, $EXP_{U,j}$ is the residential consumption expenditure in province j, $GDP_{U,j}$ represents the GDP from urban areas in province j, $P_{U,j}$ represents the urban population in province j, and P_j is the total population in province *j*. $EI_{U,i,j} = \frac{FE_{U.i,\mathrm{j}}}{Con_{U,i,j}}$ represents the emission intensity from the entire food supply chain of food i in province *j*'s urban residential consumption; $CS_{U,i,j} = \frac{Con_{U,i,j}}{Con_{U,j}}$ denotes the consumption structure of food i in province j's urban residential consumption; $CP_{U,j} = \frac{Con_{U,j}}{FEXP_{U,j}}$ denotes the purchasing power of food *i* in province *j*'s urban residential consumption (which represents the reciprocal of food price); $EN_{U,j} = \frac{FEXP_{U,j}}{EXP_{U,j}}$ is the Engel coefficient of urban residents in province *j*; $CE_{U,j} = \frac{EXP_{R,j}}{GDP_{R,j}}$ is the consumption expenditure of urban residents in province *j*; $ES_{U,j} = \frac{GDP_{U,j}}{P_{U,j}}$ is the economic development of urban area in province *j*; and $UR_{U,j} = \frac{P_{U,j}}{P_j}$ represents the urbanization ratio of province *j*.

$$\Delta FE_U = FE_U^T - FE_U^0$$
$$= \Delta FE_{U,EI} + \Delta FE_{U,CS} + \Delta FE_{U,CP} + \Delta FE_{U,EN} + \Delta FE_{U,CE} + \Delta FE_{U,ES} + \Delta FE_{U,UR} + \Delta FE_{U,P} \quad \text{Equation 4-4}$$

$$\Delta FE_R = FE_R^T - FE_R^0$$
$$= \Delta FE_{R,EI} + \Delta FE_{R,CS} + \Delta FE_{R,CP} + \Delta FE_{R,EN} + \Delta FE_{R,CE} + \Delta FE_{R,ES} + \Delta FE_{R,UR} + \Delta FE_{R,P} \quad \text{Equation 4-5}$$

where FE_U^T and FE_U^0 represent the GHGs from urban residential consumption in period *T* and the baseline period, respectively. ΔFE_U denotes the change in GHGs from urban residential consumption between period *T* and the baseline period. $\Delta FE_{U,EI}$, $\Delta FE_{U,CS}$, $\Delta FE_{U,CP}$, $\Delta FE_{U,EN}$, $\Delta FE_{U,CE}$, $\Delta FE_{U,ES}$, $\Delta FE_{U,UR}$, and $\Delta FE_{U,P}$ indicate the contributions from technology, food consumption structure, purchasing power, Engel coefficient, expenditure, economic development, urbanization and population, respectively.

Scenario Analyses

Using decomposition analysis, this study formed a multi-side (i.e., supply, demand, and socioeconomic) driven model to detect the determinants of food system GHG emissions and their spatial variability across China (Supplementary S2.1 for details). Subsequently, the study compared the emission reduction potential of different factors based on the business-as-usual scenario (BAU). It is acknowledged that some extreme events (such as the Sino-US trade war in 2018 or COVID-19) may cause shocks to economic growth. In general, however, these shocks tend to be short-term disruptions, and the long-time series scenarios employed in this study accommodate these uncertainties.

The S0 BAU scenario following SSP2, which is regarded as the most consistent with the current development trend (O'Neill et al., 2014; Fricko et al., 2017), was adopted in this study. SSP (Shared Socioeconomic Path) was developed with the comprehensive consideration of population, economy, technological progress, resource utilization and other factors, and has been used to quantitatively describe the relationship between climate change and socioeconomic development pathways (Kriegler et al., 2010; Zhang et al., 2015). SSP2 describes a scenario with a gradual reduction in dependence on fossil fuels and in which China will maintain current levels of population growth, fertility, mortality, migration, and education. It is considered that China's population will peak at 1.4 billion around 2035, the urbanization rate will peak at 80% by 2050, and population will be 1.36 billion in 2060 (Supplementary S3.1 for details). This study revised the population data for 2020 based on China's recent (2021) seventh population census. Including the SSP population forecast and urbanization rate (Gao and Wei, 2013; Pan and Shan, 2019) in the LMDI decomposition model causes China's food system GHGs to peak at 1.60 Gt CO2eq in around 2040 and then decrease to 1.54 Gt CO_2eq in 2060 (a figure that is 1.0% lower than that of 2018).

The S1 TECH scenario was based on a meta-analysis of a range of food production types in China and worldwide and a comparison of the footprint gap in food production between China and world's best-practice low-carbon production technology. A total of 352 articles in Chinese and English were identified in the determination of China's emissions, of which 217 articles were valid. The GHGs emission intensities of other countries were derived from the database provided by Clune et al. (2017) with 1,731 estimates of emissions being selected to match the carbon footprint of different types of food. It was considered that China will achieve the world's best practice technology for food production in around 2060 resulting in emissions reduction of about 173 Mt CO_2e, about 15.1% of the total emission under BAU in 2060 (see S3.2 for details).

The S2 DIET scenario was based on the Dietary Guidelines for Chinese Residents issued by the Chinese Nutrition Society (CNS, 2016). Shifts in diet driven by consumption scale and structure are key factors affecting food system GHGs emissions. Given that there are upper and lower recommended intake values for different types of food, the values in brackets are the upper and lower range of the resulting carbon emissions of dietary shifts. Under this scenario, we consider the dietary pattern will follow the Dietary Guidelines by 2060. Whole grain consumption are projected to increase by 1.8% [-21.1%-24.8%] with the intake of tubers like potato and beans increasing by 31.9% [9.9%-53.9%] by 2060. Over the same period meat consumption will reduce by 40.2% [22.1%,58.4%], whilst aquatic-derived foods will increase by 84.3% [28.2%,140.4%], eggs by 69.3% [50.5%, 88.1%], vegetables by 51.9% [13.9%, 89.9%], and fruit by 92.7% [40.1%, 145.2%]. According to this nutrient-oriented transformation of food consumption structure (i.e., reduced consumption of meat, moderate increase in whole grains, increase in fruit, vegetable, aquatic and protein products, and moderate increase in dairy products), it is estimated that China's food system GHGs emissions have the best mitigation potential of 14.9%, but there is large uncertainty [-43.0%, 7.3%] without details of the carbon-nutrient combined dietary guideline (see S3.3 for details).

The S3 SPAT scenario was based on the optimization of production location. Due to the spatial differences in climate, soils, and farm management practice (energy use, fertilizer application; Poore and Nemecek, 2018), there are regional variations in the carbon footprint of agricultural production (Vermeulen et al., 2012). As a result, regional-specific mitigation measures are needed (Liu et al., 2021) (Fig. S4). This scenario was based on identifying a spatial optimization pathway from the supply-side by adjusting agricultural production patterns and optimizing cropland expansion. The objective was to find the overall lowest GHG emissions whilst meeting the existing consumption demand, considering the potential of cropland expansion in low-carbon undeveloped areas and minimizing the transportation of crop between regions. The results showed that GHGs emissions of rice, wheat and maize production system can be reduced by 21.76%, 10.20% and 1.71%, respectively, by optimizing the distribution of production location (see S3.4 for details of the spatial equilibrium model).

The S4 IMPO scenario was based on the optimization of food imports. According to the OECO-FAO datasets (https://stats.oecd.org/index.aspx?queryid=71240), China's imports of livestock, poultry, meat and dairy products are expected to increase. This study extended the projected trends of OECD-FAO from 2025 to 2060. Livestock and poultry food imports are projected to rise by 24.8% and dairy imports by 27.7% when comparing 2025 with 2018. These increases continue into the future, and by 2060 are projected to be 1.56 times and 1.87 times, respectively, of those in 2018. By selecting countries with low production emission intensity and sufficient export capacity, China's food system GHGs emissions can be further mitigated. It is estimated that by 2050 China could mitigate 7.48 Mt CO_2eq by importing livestock and poultry and 1.89 Mt CO2eq by importing milk from green source importing countries. Pursuing this approach for another decade (i.e., figures for 2060) would lead to further mitigation (9.77 Mt CO_2eq by importing livestock and poultry and 2.49 Mt CO_2eq by importing milk; see S3.5 for details).

Limitations and uncertainty

In common with many studies, this research has some limitations. For the emissions inventory, the parameters used for the processing, wholesale and retail stages were primarily based on ESU World Food. The emission factor from cooking was adopted from food consumption survey data in the UK (Frankowska et al., 2020) and modified based on China's energy emission factors (see Table S9 for detailed references), which led to a higher proportion of emissions from retailing and cooking. In the process of data collection, parameters for different foods, regions and time series were considered with all available data (Table S4), but spatially uniform parameters were still required in some stages. More work is still needed to establish China's own food system GHG factors. In terms of the food lifecycle system boundary, due to the limited data for China's food loss and waste (FLW) and food disposal, these two stages were excluded from this study. Recent research has shown that the total amount of food lost and wasted across China's food supply chain is 350 million tons, or 27% of the total food produced (directly for consumer consumption; Li, et al., 2021). In addition, it is difficult to link LULUC with food type, and the system boundary of this study also excludes land use emissions. The emissions from LULUC associated with agricultural production (IPCC sector 3a) accounts for about 32% of global food-system emissions (Crippa et al., 2021) with drained organic soils on agricultural land dominating these emissions (Cooper et al., 2020). As a result, LULUC-related emissions could represent another factor underestimated in this study. All of these factors discussed above could drive the accounting results to be lower than current national-level estimates in Table S2. However, even with the imprecise emission parameters and uncertainties along the food supply chain, the trends of GHG emissions from the food system calculated in this study are consistent with those of the sectoral emission inventory developed by the EU (Crippa et al., 2021).

The uncertainty analysis in this study follows the IPCC Guidelines for National Greenhouse Gas Inventories for good practices and uncertainty management (2006). Uncertainties in the emissions from the production stage of the flood lifecycle mainly come from regional differences in activity survey data collected in the production process (for example, those describing fertilizer and energy use). The uncertainties in the processing and retail stages are primarily derived from the emission factors in the literature or the LCA database. Uncertainties in the transportation stage mainly come from the spatial allocation of food transport emissions by rail and road based on transport statistical data. The surveyed consumption activity data for different regions are the main source of uncertainties for the consumption stage.

After identifying the sources of each uncertainty, the CI was set at 95%; thus, the probability density function was between the 25th and 95th percentiles. Firstly, by establishing the empirical distribution functions of individual activity and emission factors, alternative probability density function models were evaluated and selected to represent the variability in activity data or emission factor data. The general probability density function distributions include normal distribution, lognormal distribution, and trigonometric distribution. Secondly, the Monte Carlo method was used to calculate (1,000 times) the established probability density function, and the range of the 95% CI was calculated to identify the uncertainty for each food type in different stages. In addition, under the IPCC Guidelines for National Greenhouse Gas Inventories for good practices and uncertainty management (IPCC, 2006), all uncertainties can be combined and transmitted through two types of methods. The first is applicable to the merger between two unrelated emission sources (Equation 4-6), and the second applies to the merger between two related emission sources (Equation 4-7), with the following formula:

$$U_{total} = \sqrt{U_1^2 + U_2^2 + U_3^2 + \cdots + U_n^2}, \ \ \text{i=1…n} \qquad \text{Equation 4-6}$$

$$U_{total} = \sqrt{\frac{(U_1 * x_1)^2 + (U_2 * x_2)^2 + \cdots + (U_n * x_n)^2}{(x_1 + x_2 + \cdots + x_n)^2}}, \ \ \text{i=1…n} \qquad \text{Equation 4-7}$$

where U_{total} is the combined uncertainty, U_i is the uncertainty of each functional unit, and x_i is the activity value of each unit.

References

Ang, B. W. (2004). Decomposition analysis for policymaking in energy: which is the preferred method? Energy policy, 32(9), 1131-1139.

Bai, Z., Fan, X., Jin, X., Zhao, Z., Wu, Y., Oenema, O., Velthof, G., Hu, C., Ma, L. (2022). Relocate 10 billion livestock to reduce harmful nitrogen pollution exposure for 90% of China's population. Nature Food, 3(2), 152-160.

Bajželj, B., Richards, K. S., Allwood, J. M., Smith, P., Dennis, J. S., Curmi, E., & Gilligan, C. A. (2014). Importance of food-demand management for climate mitigation. Nature Climate Change, 4(10), 924-929.

CNS (Chinese Nutrition Society) (2016). The Chinese Dietary Guidelines. http://dg.cnsoc.org/article/04/8a2389fd5520b4f30155be1475e02741.html

Crippa, M., Solazzo, E., Guizzardi, D., Monforti-Ferrario, F., Tubiello, F. N., & Leip, A. (2021). Food systems are responsible for a third of global anthropogenic GHG emissions. Nature Food, 2(3), 198-209.

Cui, Z., Zhang, H., Chen, X., Zhang, C., Ma, W., Huang, C., Zhang, W., Mi, G., Miao, Y., Li, X., Gao, Q., Yang, J., Wang, Z., Ye, Y., Guo, S., Lu, J., Huang, J., Lv, S., Sun, Y., Liu, Y., Peng, X., Ren, J., Li, S., Deng, X., Shi, X., Zhang, Q., Yang, Z., Tang, L., Wei, C., Jia, L., Zhang, J., He, M., Tong, Y., Tang, Q., Zhong, X., Liu, Z., Cao, N., Kou, C., Ying, H., Yin, Y., Jiao, X., Zhang, Q., Fan, M., Jiang, R., Zhang, F., Dou, Z. (2018). Pursuing sustainable productivity with millions of smallholder farmers. Nature, 555(7696), 363-366.

Cooper, H. V., Evers, S., Aplin, P., Crout, N., Dahalan, M. P. B., & Sjogersten, S. (2020). Greenhouse gas emissions resulting from conversion of peat swamp forest to oil palm plantation. Nature communications, 11(1), 1-8.

Nature Editorial. The war in Ukraine is exposing gaps in the world's food-systems research. Nature 604, 217-218 (2022) .doi: https://doi.org/10.1038/d41586-022-00994-8

EU (European Union). Farm to Fork Strategy. (2020). https://ec.europa.eu/food/farm2fork_en

FAO. (2006) Livestock's long shadow. Rome, Italy. http://www.fao.org/3/a0701e/a0701e00.htm

Fan, S. (2021). Economics in food systems transformation. Nature Food, 2(4), 218-219.

Frank, S., Havlík, P., Stehfest, E., van Meijl, H., Witzke, P., Pérez-Domínguez, I., van Dijk, M., Doelman, J.C. Fellmann, T., Koopman, J.F.L., Tabeau, A. Valin, H. (2019). Agricultural non-CO_2 emission reduction potential in the context of the 1.5℃ target. Nature Climate Change, 9(1), 66-72.

Frankowska, A., Rivera, X. S., Bridle, S., Kluczkovski, A. M. R. G., da Silva, J. T., Martins, C. A., Rauber, F., Levy, R.B., Cook, J. Reynolds, C. (2020). Impacts of home cooking methods and appliances on the GHG emissions of food. Nature Food, 1(12), 787-791.

Fricko, O., Havlik, P., Rogelj, J., Klimont, Z., Gusti, M., Johnson, N., Peter K., Manfred S., Hugo, V., Markus A., Tatiana, E., Nicklas, F., Mario, He., Chris, H., Georg K., Volker, Krey., David L. McCollum, D.L., Michael, O., Shonali, P., Shilpa, R., Erwin, S., Wolfgang, S., Riahi, K. (2017). The marker quantification of the Shared

Socioeconomic Pathway 2: A middle-of-the-road scenario for the 21st century. Global Environmental Change, 42, 251-267.

Fujimori, S., Wu, W., Doelman, J., Frank, S., Hristov, J., Kyle, P., Ronald Sands, R., van Zeist, W.J., Havlik, P., Domínguez, I.P., Sahoo, A., Stehfest, E., Tabeau, A., Valin, H., van Meijl, H., Hasegawa, T., Takahashi, K. (2022). Land-based climate change mitigation measures can affect agricultural markets and food security. Nature Food, 3(2), 110-121.

Garnett, T. (2008). Cooking up a storm: Food, greenhouse gas emissions and our changing climate. Food Climate Research Network, Centre for Environmental Strategy, University of Surrey.

Garnett, T. (2011). Where are the best opportunities for reducing greenhouse gas emissions in the food system (including the food chain) ? Food policy, 36, S23-S32.

Garnett, T. (2015) Overview of changes and drivers in China's food system. in Garnett, T. & Wilkes, A (edit) Appetite for change Social, economic and environmental transformations in China's food system. University of Oxford, Oxford, the UK.

Godfray, H. C. J., Beddington, J. R., Crute, I. R., Haddad, L., Lawrence, D., Muir, J. F., Jules Pretty, J., Robinson, S., Thomas, S.M., Toulmin, C. (2010). Food security: the challenge of feeding 9 billion people. Science, 327(5967), 812-818.

Godfray, H. C. J., Aveyard, P., Garnett, T., Hall, J. W., Key, T. J., Lorimer, J., Ray T. Pierrehumbert, R.T., Scarborough, P., Springmann, M., Jebb, S. A. (2018). Meat consumption, health, and the environment. Science, 361(6399).

Gustafson, D., Asseng, S., Kruse, J., Thoma, G., Guan, K., Hoogenboom, G., Marty Matlock, M., McLean, M., Parajuli, R., Rajagopalan, K., Stöckle, C., Sulser, T.B., Tarar, L., Wiebe, K., Zhao, C., Fraisse, C., Gimenez, C., Intarapapong, P., Karimi, T., Kruger, C., Li, Y., Marshall, E., Nelson, R.L., Pronk, A., Raymundo, R., Riddle, A.A., Rosenbohm, M., Sonke, D., van Evert, F., Wu G., Xiao, L. (2021). Supply chains for processed potato and tomato products in the United States will have enhanced resilience with planting adaptation strategies. Nature Food, 2(11), 862-872.

Hasegawa, T., Fujimori, S., Havlík, P., Valin, H., Bodirsky, B. L., Doelman, J. C., Fellmann, T., Kyle, P., Koopman, J.F.L., Lotze-Campen, H., Mason-D'Croz, D., Ochi, Y., Domínguez, I.P., Stehfest, E., Sulser, T.B., Tabeau, A., Takahashi, K., Takakura, J., van Meijl, H., van Zeist, W.J., Wiebe K., Witzke, P. (2018). Risk of increased food insecurity under stringent global climate change mitigation policy. Nature Climate Change, 8(8), 699-703.

Hayek, M. N., Harwatt, H., Ripple, W. J., & Mueller, N. D. (2021). The carbon opportunity cost of animal-sourced food production on land. Nature Sustainability, 4(1), 21-24.

Heller, M. C., & Keoleian, G. A. (2015). Greenhouse gas emission estimates of US dietary choices and food loss. Journal of Industrial Ecology, 19(3), 391-401.

He, P., Baiocchi, G., Hubacek, K., Feng, K., & Yu, Y. (2018). The environmental impacts of rapidly changing diets and their nutritional quality in China. Nature Sustainability, 1(3), 122-127.

He, P., Feng, K., Baiocchi, G., Sun, L., & Hubacek, K. (2021). Shifts towards healthy diets in the US can reduce environmental impacts but would be unaffordable for poorer minorities. Nature Food, 2(9), 664-672.

Hu, Y., Su, M., Wang, Y., Cui, S., Meng, F., Yue, W., Liu, Y., Xu C., Yang, Z. (2020). Food production in China requires intensified measures to be consistent with national and provincial environmental boundaries. Nature Food, 1(9), 572-582.

IPCC. IPCC Guidelines for National Greenhouse Gas Inventories. (2006) https://www.ipcc.ch/report/2006-ipcc-guidelines-for-national-greenhouse-gas-inventories/ [2006-5-1]

IPCC. Climate change and land: an IPCC special report on climate change, desertification, land degradation, sustainable land management, food security, and greenhouse gas fluxes in terrestrial ecosystems. (2019) https://www.ipcc.ch/site/assets/uploads/sites/4/2020/02/SPM_Updated-Jan20.pdf [2019-10-30].

IPCC. Mitigation of Climate Change, IPCC Six Assessment Report, Climate Change 2022: (2022) https://www.ipcc.ch/report/sixth-assessment-report-working-group-3/ [2022-4-4].

Jin S., Zhang B., Wu B., Han D., Hu Y., Ren C., Zhang C., Wei X., Wu Y., Mol Arthur P. J., Reis S., Gu B., Chen J. (2020) Decoupling livestock and crop production at the household level in China. Nature Sustainability, 4, 48-55. doi:10.1038/s41893-020-00596-0.

Kehlbacher, A., Tiffin, R., Briggs, A., Berners-Lee, M., & Scarborough, P. (2016). The distributional and nutritional impacts and mitigation potential of emission-based food taxes in the UK. Climatic Change, 137(1), 121-141.

Kramer, K. J., Moll, H. C., Nonhebel, S., & Wilting, H. C. (1999). Greenhouse gas emissions related to Dutch food consumption. Energy Policy, 27(4), 203-216.

Lai, L., Huang, X., Yang, H., Chuai, X., Zhang, M., Zhong, T., Chen, Z., Chen, Y., Wang, X., Thompson, J. R. 2016, Carbon emissions from land-use change and management in China between 1990 and 2010. Science Advances 2, (11), e1601063. DOI: 10.1126/sciadv.1601063

Li, Y., Wang, L. E., Liu, G., & Cheng, S. (2021). Rural household food waste characteristics and driving factors in China. Resources, Conservation and Recycling, 164, 105209.

Liu, Z., Ying, H., Chen, M., Bai, J., Xue, Y., Yin, Y., Batchelor, W.D., Yang, Y., Bai, Z., Du, M., Guo, Y., Zhang, Q., Cui, Z., Zhang, F., Dou, Z. (2021). Optimization of China's maize and soy production can ensure feed sufficiency at lower nitrogen and carbon footprints. Nature Food, 2, 426-433.

Poore, J., & Nemecek, T. (2018). Reducing food's environmental impacts through producers and consumers. Science, 360(6392), 987-992.

Roe, S., Streck, C., Obersteiner, M., Frank, S., Griscom, B., Drouet, L., Fricko, O., Gusti, M., Harris, N., Hasegawa, T., Hausfather, Z., Havlík, P., House, J., Nabuurs, G.J., Popp, A., José Sanz Sánchez, M., Sanderman, J., Smith, P., Stehfest, E., Lawrence, D. (2019). Contribution of the land sector to a 1.5 C world. Nature Climate Change, 9(11), 817-828.

Rosenzweig, C., Mbow, C., Barioni, L. G., Benton, T. G., Herrero, M., Krishnapillai, M., Liwenga, E.T., Pradhan, P., Rivera-Ferre, M.G., Sapkota, T., Tubiello, F.N., Xu, Y., ContrerasE.M., Portugal-Pereira, J. (2020). Climate change responses benefit from a global food system approach. Nature Food, 1(2), 94-97.

Rosenzweig, C., Tubiello, F. N., Sandalow, D., Benoit, P., & Hayek, M. N. (2021). Finding and fixing food system emissions: the double helix of science and policy. Environmental Research Letters, 16(6), 061002

Springmann, M., Clark, M., Mason-D'Croz, D., Wiebe, K., Bodirsky, B. L., Lassaletta, L., & Willett, W. (2018). Options for keeping the food system within environmental limits. Nature, 562(7728), 519-525.

Soergel, B., Kriegler, E., Bodirsky, B. L., Bauer, N., Leimbach, M., & Popp, A. (2021). Combining ambitious climate policies with efforts to eradicate poverty. Nature communications, 12(1), 1-12.

Sun, Z., Scherer, L., Tukker, A., Spawn-Lee, S. A., Bruckner, M., Gibbs, H. K., & Behrens, P. (2022). Dietary change in high-income nations alone can lead to substantial double climate dividend. Nature Food, 3, 29-37.

Tubiello, F. N., Rosenzweig, C., Conchedda, G., Karl, K., Gütschow, J., Pan. X., Obli-Laryea, G., Wanner, N., Qiu, S.Y., Barros, J.D., Flammini, A., Mencos-Contreras, E., Souza, L., Quadrelli, R., Heiðarsdóttir, H.H., Benoit, P., Hayek M., Sandalow, D. (2021). Greenhouse gas emissions from food systems: building the evidence base. Environmental Research Letters, 16(6), 065007.

Tubiello, F. N., Karl, K., Flammini, A., Gütschow, J., Obli-Layrea, G., Conchedda, G., Pan, X., Qi, S.Y., Heiðarsdóttir, H.H., Wanner,. N., Quadrelli, R., Souza, L.R., Benoit, P., Hayek. M., Sandalow, D., Contreras, E.M., Rosenzweig, C., Moncayo, J.R., Conforti, P/. Torero, M. (2021). Pre-and post-production processes along supply chains increasingly dominate GHG emissions from agri-food systems globally and in most countries. Earth System Science Data Discussions, 14, 1795-1809.

UN (United Nations). (2016). Progress Towards the Sustainable Development Goals. https://sdgs.un.org/goals

Vermeulen, S. J., Campbell, B. M., & Ingram, J. S. (2012). Climate change and food systems. Annual review of environment and resources, 37, 195-222.

Xue, L., Liu, X., Lu, S., Cheng, G., Hu, Y., Liu, J., Dou, Z., Cheng, S., Liu, G. (2021). China's food loss and waste embodies increasing environmental impacts. Nature Food, 2, 519-528.

Zhao, H., Chang, J., Havlík, P., van Dijk, M., Valin, H., Janssens, C., Ma, L., Bai, Z., Herrero, M., Smith, P., & Obersteiner, M. (2021). China's future food demand and its implications for trade and environment. Nature Sustainability, 4, 1042-1051.

Zhang, W. F., Dou, Z. X., He, P., Ju, X. T., Powlson, D., Chadwick, D., David Norsee, D., Lu, Y.L., Zhang, Y., Wu, L., Chen, X.P., Cassman, K.G., Zhang, F. S. (2013). New technologies reduce greenhouse gas emissions from nitrogenous fertilizer in China. Proceedings of the National Academy of Sciences, 110(21), 8375-8380.

Supplementary Files

This is a list of supplementary files associated with this preprint. Click to download.

- AppendixCuttingcarbonemissionsfromChinafood.docx